

12-2007

Exchange Bias in Bulk Mn Rich Ni–Mn–Sn Heusler Alloys

Mahmud Khan

Southern Illinois University Carbondale

Igor Dubenko

Southern Illinois University Carbondale

Shane Stadler

Southern Illinois University Carbondale

Naushad Ali

Southern Illinois University Carbondale

Follow this and additional works at: http://opensiuc.lib.siu.edu/phys_pubs

© 2007 American Institute of Physics

Published in *Journal of Applied Physics*, Vol. 102 No. 11 (2007) at doi: [10.1063/1.2818016](https://doi.org/10.1063/1.2818016)

Recommended Citation

Khan, Mahmud, Dubenko, Igor, Stadler, Shane and Ali, Naushad. "Exchange Bias in Bulk Mn Rich Ni–Mn–Sn Heusler Alloys." (Dec 2007).

This Article is brought to you for free and open access by the Department of Physics at OpenSIUC. It has been accepted for inclusion in Publications by an authorized administrator of OpenSIUC. For more information, please contact opensiuc@lib.siu.edu.

Exchange bias in bulk Mn rich Ni–Mn–Sn Heusler alloys

Mahmud Khan,^{a)} Igor Dubenko, Shane Stadler, and Naushad Ali
Department of Physics, Southern Illinois University, Carbondale, Illinois 62901, USA

(Received 19 September 2007; accepted 4 October 2007; published online 11 December 2007)

An experimental study on the exchange bias properties of bulk polycrystalline $\text{Ni}_{50}\text{Mn}_{50-x}\text{Sn}_x$ Heusler alloys has been performed. Martensitic transformations have been observed in the alloys for some critical Sn concentrations. The alloys, while in their respective martensitic phases, are found to exhibit exchange bias effect. Shifts in hysteresis loops of up to 225 Oe were observed in the 50 kOe field cooled samples. The observed exchange bias behavior in $\text{Ni}_{50}\text{Mn}_{50-x}\text{Sn}_x$ is attributed to the coexistence of antiferromagnetic and ferromagnetic exchange interactions in the system.

© 2007 American Institute of Physics. [DOI: 10.1063/1.2818016]

INTRODUCTION

The exchange bias (EB) phenomenon is usually described as the shift of the magnetic hysteresis loop of a material from the origin when it is cooled in the presence of an applied magnetic field. Since its discovery in 1956,¹ extensive research has been conducted on this subject, both experimentally and theoretically, which resulted in the observation of EB properties in many magnetic materials.^{2–11} The discovery of such materials opened new doors of technological applications that resulted in the outcome of technological devices including permanent magnets,^{8,10} magnetic recording media,⁹ sensors, read heads, and many others.⁸ The observation of EB effect is usually attributed to the ferromagnetic (FM)-antiferromagnetic (AFM) interfaces present in an EB material. The phenomenon is generally observed in small oxide coated particles, inhomogeneous materials, and thin films.^{8,9}

EB properties are also found to exist in certain bulk systems,^{12,13} but such observations are very rare, and therefore from both scientific and application points of view bulk materials exhibiting EB properties are of intense interest.

In recent years, Mn rich $\text{Ni}_{50}\text{Mn}_{50-x}\text{Y}_x$ ($Y=\text{Sb}, \text{Sn},$ and In) Heusler alloy systems have revealed tremendous potential from application point of view. For some critical range of Y concentration these alloy systems are found to undergo martensitic phase transformation from a high temperature cubic phase (austenite) to a low temperature orthorhombic phase (martensite). Since it was reported by Sutou *et al.*,¹⁴ quite a few experimental work on this system, which revealed many of its promising properties, including large magnetic entropy changes, and giant magnetoresistance, have been reported.^{15–18} Detailed studies on the magnetic and structural properties of these systems have also been reported.^{19,20} Recently, observation of EB in a bulk Ni–Mn–Sb based Heusler alloy system was reported.²¹

In this work, we report the observation of EB in the bulk polycrystalline $\text{Ni}_{50}\text{Mn}_{50-x}\text{Sn}_x$ Heusler alloy system. A detailed systematic study on the EB properties of this system has been performed.

EXPERIMENTAL TECHNIQUE

A conventional arc melting method was used to fabricate approximately 5 g polycrystalline buttons of $\text{Ni}_{50}\text{Mn}_{50-x}\text{Sn}_x$ ($10 \leq x \leq 17$). The weight loss of the resulting alloy, after melting, was found to be less than 0.2%. To homogenize the samples, they were wrapped in a Ta foil and annealed in vacuum for 24 h at 850 °C, and slowly cooled down to room temperature.

Room temperature x-ray diffraction measurements were performed using a minimaterials analyzer (MMA) x-ray diffractometer made by GBC Scientific Equipment, Inc. The diffractometer employed $\text{Cu K}\alpha$ radiation and Bragg-Brentano geometry.

Magnetization measurements were done using a superconducting quantum interference device (SQUID) magnetometer made by Quantum Design, Inc. The measurements were performed in a temperature range of 5–400 K and in magnetic fields up to 5 T. For zero field cooled (ZFC) measurements, the samples were cooled down from 380 to 5 K in zero magnetic field. For field cooled (FC) measurements, the samples were cooled down to 5 K from 380 K in applied magnetic fields ranging from 0.01 to 5 T.

RESULTS AND DISCUSSION

Room temperature x-ray diffraction (XRD) patterns of all the $\text{Ni}_{50}\text{Mn}_{50-x}\text{Sn}_x$ samples suggest that the samples are of single phase and possess cubic $L2_1$ ($14 \leq x \leq 17$) and orthorhombic ($11 \leq x \leq 13$) structures. In Fig. 1 the ZFC and FC magnetization as a function of temperature curves [$M(T)$], of $\text{Ni}_{50}\text{Mn}_{50-x}\text{Sn}_x$ ($11 \leq x \leq 17$), measured in a 100 Oe field, are shown. Figure 1(a) shows a magnetic transition in the ZFC curve of the alloy with $x=11$ at around 75 K. Since the EB effect vanishes below this temperature, we refer to this transition temperature as the conventional exchange bias blocking temperature, T_B . However, for further confirmation of this temperature being the blocking temperature, the magnetic structures of the $\text{Ni}_{50}\text{Mn}_{50-x}\text{Sn}_x$ system need to be determined. With further increase of temperature, a ferromagnetic transition was observed at around 155 K. This temperature is defined as T_C^M and represents the ferromagnetic Curie temperature of the martensitic phase.^{19,20} In the alloy with $x=12$, $T_B \approx 135$ K and T_C^M is observed near

^{a)}Author to whom correspondence should be addressed. Electronic mail: mkhan@siu.edu.

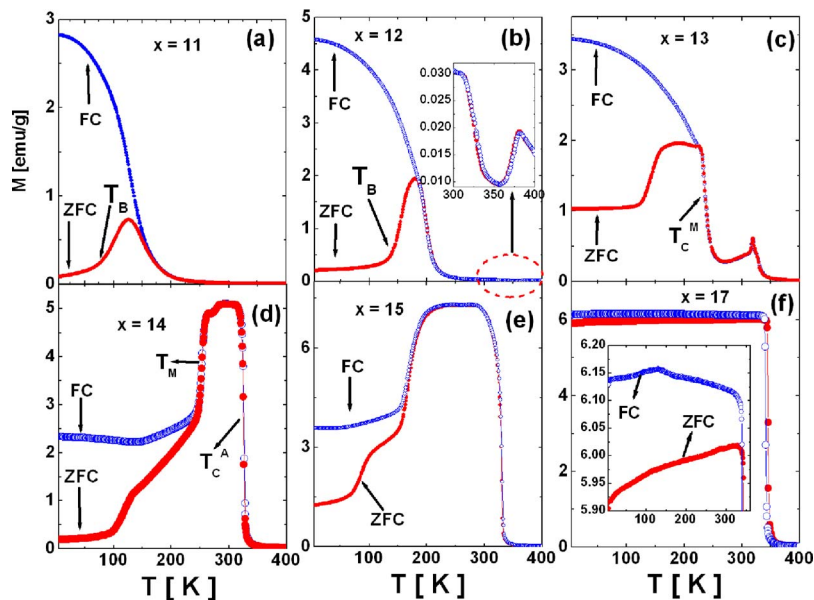


FIG. 1. (Color online) Zero field cooled (ZFC) and field cooled (FC) magnetization curves as a function of temperature of $\text{Ni}_{50}\text{Mn}_{50-x}\text{Sn}_x$, obtained at a field of 0.01 T. The inset of (b) shows the magnified portion of the circled part of the figure.

195 K. Up to this temperature, the only transition observed in the FC curve of the alloy with $x=12$ is the ferromagnetic transition at T_C^M . Below 185 K the ZFC and FC curves split indicating irreversible behavior.

With further increased temperature, an antiferromagnetic-type transition was observed in both ZFC and FC curves near 365 K [see the inset of Fig. 1(b)]. This transition appears more clearly in the $M(T)$ curves of the alloys with $x=13$ at around 315 K [see Fig. 1(c)]. This transition temperature represents the martensitic transition temperature T_M .¹² Below this martensitic transition temperature, the alloy with $x=13$ exhibits similar behavior to that of the alloy with $x=12$. The martensitic transformation becomes more clear in the alloy with $x=14$, as shown in Fig. 1(d). At near 328 K a ferromagnetic transition is observed in the alloy with $x=14$. This transition temperature is the ferromagnetic Curie temperature, T_C^A , of the austenitic phase.

The martensitic transformation is observed for $x \leq 16$ and no martensitic transformation is observed in the alloy with $x=17$. It is noticeable in Fig. 1 that, in the alloys with $x \leq 13$, the ZFC and FC $M(T)$ curves show irreversible (splitting between ZFC and FC curves) behavior below T_C^M , and for the alloys with $14 \leq x \leq 16$, the irreversible behavior is observed below T_M . ZFC and FC $M(T)$ curves of the alloy with $x=17$ show irreversible behavior below T_C^A . The splitting of the ZFC and FC $M(T)$ curves can be explained by the coexistence of ferromagnetic and antiferromagnetic interactions in the $\text{Ni}_{50}\text{Mn}_{50-x}\text{Sn}_x$ system.^{19,20} The antiferromagnetic interaction arises from the antiferromagnetic coupling between Mn atoms in the Mn sites, and the Mn atoms that occupied the Sn sites.

Due to the presence of mixed magnetic regions, cooling under the influence of a magnetic field produces a magnetic domain structure that is different than the domain structure

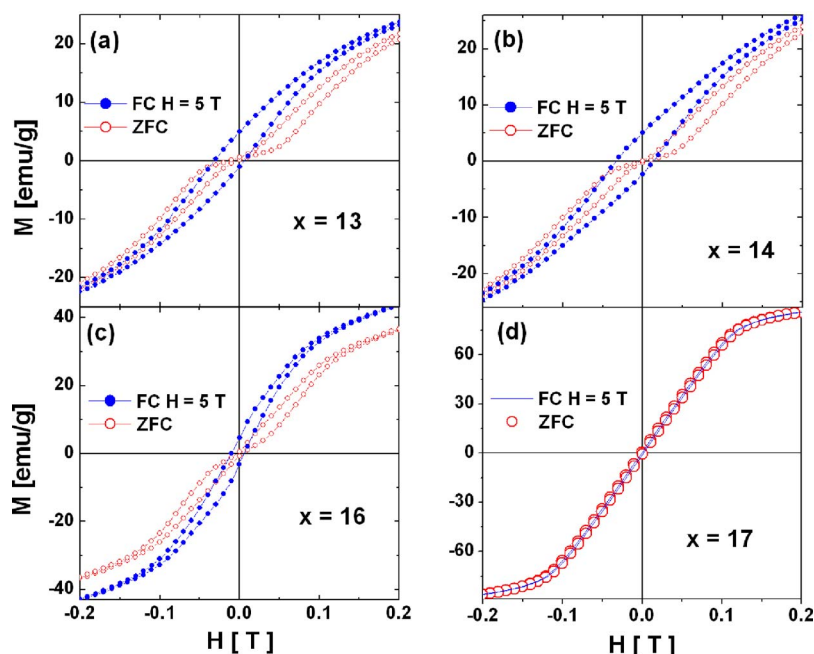


FIG. 2. (Color online) Zero field and 5 T field cooled magnetization curves as a function of field for $\text{Ni}_{50}\text{Mn}_{50-x}\text{Sn}_x$ obtained at 5 K.

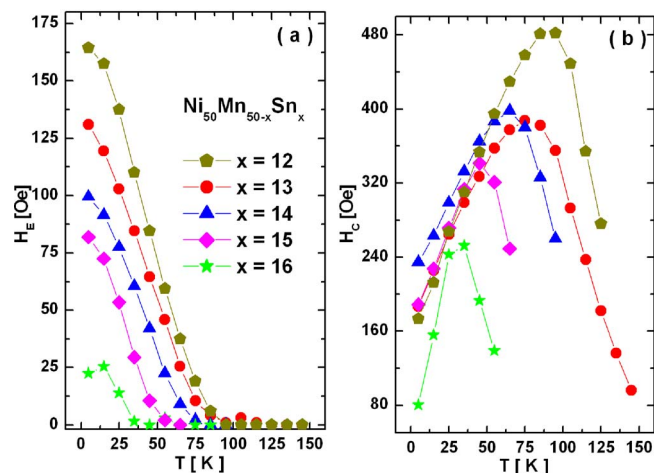


FIG. 3. (Color online) (a) Exchange bias field (H_E) and (b) coercive field (H_C) as a function of temperature of $\text{Ni}_{50}\text{Mn}_{50-x}\text{Sn}_x$.

formed when the system is zero field cooled. Figure 2 shows the ZFC and FC hysteresis loops of $\text{Ni}_{50}\text{Mn}_{50-x}\text{Sn}_x$ ($x = 13, 14, 16, 17$) from -0.2 to 0.2 T. The actual measurements were done from -2 to 2 T. For clear visualization of the loop shift, only the loop from -0.2 to 0.2 T is shown. Figure 2 shows that the FC curves of the $\text{Ni}_{50}\text{Mn}_{50-x}\text{Sn}_x$ alloys for $12 \leq x \leq 16$ shift from the origin, exhibiting the EB effect. This observation of the EB also suggests the coexistence of antiferromagnetic and ferromagnetic coupling in the system. The double-shifted loops observed in the ZFC curves of the alloys with $12 \leq x \leq 16$ also show the existence of such coupling. Such double-shifted loops are usually observed in certain EB materials with AFM and FM layers.^{22–28} During the zero field cooling process of the EB materials showing such loops, the FM layer forms a special striped-type domain structure.²⁴ Because of the uniaxial anisotropy of the FM layer, the magnetization in each striped domain becomes aligned in either of the two directions that are equally preferred, thus resulting in double-shifted hysteresis loops when cooled in the presence of zero magnetic field. The double shifted loops in the $\text{Ni}_{50}\text{Mn}_{50-x}\text{Sn}_x$ system most probably arise from a striped domain-type structure formed by the FM regions of the system. The double-shifted loops observed in the $\text{Ni}_{50}\text{Mn}_{50-x}\text{Sn}_x$ system could also be explained by exchange-spring effects.²⁸ The AFM regions form a continuous matrix such as a structure in which the FM regions get embedded in the form of clusters. This structure results in significant interfacial exchange that leads to the alignment of the FM spins by the AFM spins. In such a situation, the AFM matrix plays the role of a hard magnetic phase aligning the soft FM clusters. The cluster spin orientation is set either up or down and thus results in a double-shifted loop. Detail of this phenomenon is explained in Ref. 28.

Although some coexistence of FM and AFM interactions is also present in the alloy with $x=17$, as deduced from the splitting of the ZFC and FC $M(T)$ curves [see inset of Fig. 1(f)], no EB effect was observed in the alloy. This could mean that the antiferromagnetic coupling in the austenitic phase is too weak to give rise to such an effect. Figures 3(a) and 3(b) show the EB field (H_E) as a function of temperature

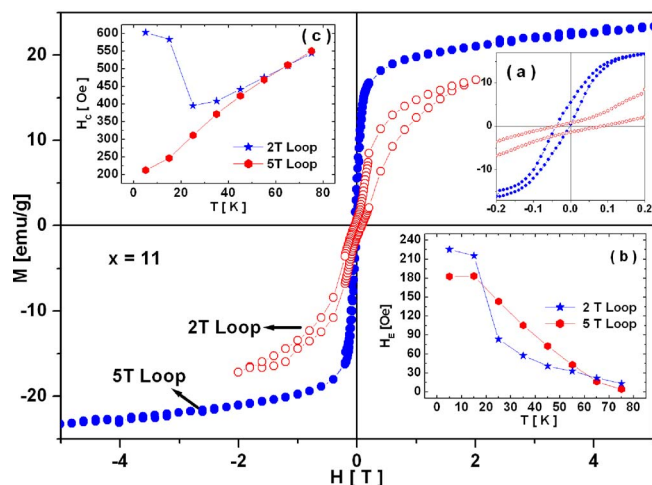


FIG. 4. (Color online) Field cooled 2 and 5 T hysteresis loops of $\text{Ni}_{50}\text{Mn}_{50-x}\text{Sn}_x$ ($x=11$). Inset (a) represents the 2 and 5 T hysteresis loops in the lower field region, (b) H_E as a function of temperature, and (c) H_C as a function of temperature of $\text{Ni}_{50}\text{Mn}_{50-x}\text{Sn}_x$ ($x=11$).

and the coercive field (H_C) as a function of temperature of $\text{Ni}_{50}\text{Mn}_{50-x}\text{Sn}_x$, respectively. In each alloy, H_E was found to decrease as the temperature approached T_B , while the coercivity first increases and then decreases as H_E diminishes. The EB effect was also observed in the alloy with $x=11$. However, the EB properties were found to be different when measurements were done in 2 and 5 T loops (see Fig. 4). The 2 T loops show larger hysteresis and corresponding larger H_E and H_C (see insets of Fig. 4). Highest H_E values of 225 Oe (2 T loop) and 183 Oe (5 T loop) were observed in the alloy with $x=11$. This dependence of exchange bias properties on the field strength of the alloy with $x=11$ could be due to minor-loop effects, which means that the sample was not properly saturated at a 2 T field. It was found that H_E in the $\text{Ni}_{50}\text{Mn}_{50-x}\text{Sn}_x$ system is inversely proportional to the saturation moment, which is a typical behavior of EB phenomena. As shown in Fig. 5, H_E decreases as the Sn concentration (x) and corresponding magnetization at 5 K increase. The decrease of H_E with increasing Sn concentration could be due to the increase of the size of the FM interface in the $\text{Ni}_{50}\text{Mn}_{50-x}\text{Sn}_x$ system.

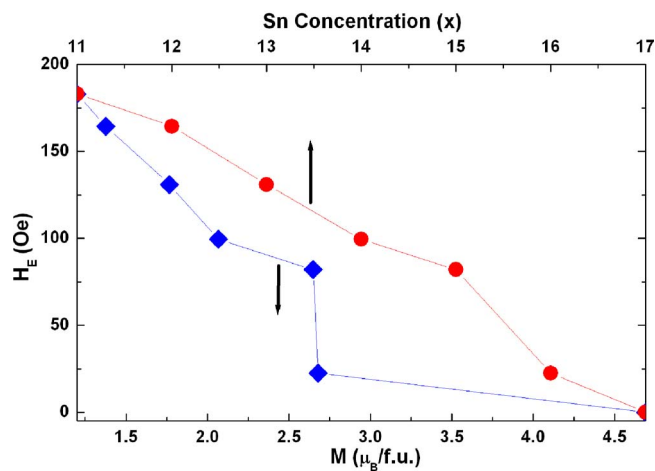


FIG. 5. (Color online) Exchange bias field (H_E) as a function of magnetization at 5 T and Sn concentration of $\text{Ni}_{50}\text{Mn}_{50-x}\text{Sn}_x$.

CONCLUSION

In summary, exchange bias behavior has been observed in bulk polycrystalline $\text{Ni}_{50}\text{Mn}_{50-x}\text{Sn}_x$ Heusler alloys. Shifts in the hysteresis loops of the samples occurred when the samples were cooled down to 5 K in an applied magnetic field of 5 T. The observed EB phenomena in $\text{Ni}_{50}\text{Mn}_{50-x}\text{Sn}_x$ are attributed AFM-FM interfaces within the system that results from the coexistence of AFM and FM exchange interactions.

ACKNOWLEDGMENTS

This research was supported by a Research Opportunity Award from Research Corporation (RA0357), and by the Office of Basic Energy Sciences, Material Sciences Division of the U.S. Department of Energy (Contract No. DE-FG02-06ER46291).

¹W. H. Meiklejohn and C. P. Bean, *Phys. Rev.* **102**, 1413 (1956).

²J. Nogués, D. Lederman, T. J. Moran, and I. K. Schuller, *Phys. Rev. Lett.* **76**, 4624 (1996).

³S. Maat, K. Takano, S. S. P. Parkin, and E. E. Fullerton, *Phys. Rev. Lett.* **87**, 087202 (2001).

⁴M. R. Fitzsimmons, C. Leighton, J. Nogués, A. Hoffmann, K. Liu, C. F. Majkrzak, J. A. Dura, J. R. Groves, R. W. Springer, P. N. Arendt, V. Leiner, H. Lauter, and I. K. Schuller, *Phys. Rev. B* **65**, 134436 (2002).

⁵M. Kiwi, *J. Magn. Magn. Mater.* **234**, 584 (2001).

⁶M. D. Stiles and R. D. McMichael, *Phys. Rev. B* **63**, 064405 (2001).

⁷U. Nowak, K. D. Usadel, J. Keller, P. Miltényi, B. Beschoten, and G. Güntherodt, *Phys. Rev. B* **66**, 014430 (2002).

⁸J. Nogués and I. K. Schuller, *J. Magn. Magn. Mater.* **192**, 203 (1999).

⁹J. C. S. Kools, *IEEE Trans. Magn.* **32**, 3165 (1996).

¹⁰J. Nogués, J. Sort, V. Langlais, V. Skumryev, S. Suriñach, J. S. Muñoz,

and M. D. Baró, *Phys. Rep.* **422**, 65 (2005).

¹¹R. L. Stamps, *J. Phys. D* **33**, R247 (2000).

¹²T. Qian, G. Li, T. Zhang, T. F. Zhou, X. Q. Xiang, X. W. Kang, and X. G. Li, *Appl. Phys. Lett.* **90**, 012503 (2007).

¹³S. Koga and K. Narita, *J. Appl. Phys.* **53**, 1655 (1982).

¹⁴Y. Sutou, Y. Imano, N. Koeda, T. Omori, R. Kainuma, K. Ishida, and K. Oikawa, *Appl. Phys. Lett.* **85**, 4358 (2004).

¹⁵M. Khan, N. Ali, and S. Stadler, *J. Appl. Phys.* **101**, 053919 (2007).

¹⁶T. Krenke, E. Duman, M. Acet, E. F. Wassermann, X. Moya, L. Mañosa, and A. Planes, *Nat. Mater.* **4**, 450 (2005).

¹⁷K. Koyama, H. Okada, K. Wantanabe, T. Kanomata, R. Kainuma, W. Ito, K. Oikawa, and K. Ishida, *Appl. Phys. Lett.* **89**, 182510 (2006).

¹⁸S. Y. Yu, Z. H. Liu, G. D. Liu, J. L. Chen, Z. X. Cao, G. H. Wu, B. Zhang, and X. X. Zhang, *Appl. Phys. Lett.* **89**, 162503 (2006).

¹⁹T. Krenke, M. Acet, E. F. Wassermann, X. Moya, L. Mañosa, and A. Planes, *Phys. Rev. B* **72**, 014412 (2005).

²⁰T. Krenke, M. Acet, E. F. Wassermann, X. Moya, L. Mañosa, and A. Planes, *Phys. Rev. B* **73**, 174413 (2006).

²¹M. Khan, I. Dubenko, S. Stadler and N. Ali, *Appl. Phys. Lett.* **91**, 072510 (2007).

²²S. Brück, J. Sort, V. Baltz, S. Surinach, J. Santiago Munoz, B. Dieny, M. DolorsBaro, and J. Nogues, *Adv. Mater. (Weinheim, Ger.)* **17**, 2978 (2005).

²³P. Miltényi, M. Gierlings, M. Bamming, U. May, G. Güntherodt, J. Nogués, C. Leighton, and I. K. Schuller, *Appl. Phys. Lett.* **75**, 2304 (1999).

²⁴N. J. Gökemeijer, J. W. Cai, and C. L. Chien, *Phys. Rev. B* **60**, 3033 (1999).

²⁵H. W. Zhao, W. N. Wang, Y. J. Wang, W. S. Zhan, and J. Q. Xiao, *J. Appl. Phys.* **91**, 6893 (2002).

²⁶C. H. Lai, S. A. Chen, and J. C. A. Huang, *J. Magn. Magn. Mater.* **209**, 122 (2000).

²⁷C. L. Chien, V. S. Gornakov, V. I. Nikitenko, A. J. Shapiro, and R. D. Shull, *Phys. Rev. B* **68**, 014418 (2003).

²⁸A. N. Dobrynin, M. J. Van Bael, K. Temst, and P. Lievens, *New J. Phys.* **9**, 258 (2007).